University of Groningen

Induced expression of P-gp and BCRP transporters on brain endothelial cells using transferrin functionalized nanostructured lipid carriers

Arduino, Ilaria ; Iacobazzi, Rosa Maria ; Riganti, Chiara; Lopedota, Angela Assunta ; Perrone, Maria Grazia; Lopalco, Antonio ; Cutrignelli, Annalisa ; Cantore, Mariangela; Laquintana, Valentino; Franco, Massimo

IMPORTANT NOTE: You are advised to consult the publisher's version (publisher's PDF) if you wish to cite from it. Please check the document version below.

Document Version
Publisher's PDF, also known as Version of record

Link to publication in University of Groningen/UMCG research database

Citation for published version (APA):
Arduino, I., Iacobazzi, R. M., Riganti, C., Lopedota, A. A., Perrone, M. G., Lopalco, A., Cutrignelli, A., Cantore, M., Laquintana, V., Franco, M., Colabufo, N. A., Luurtsema, G., Contino, M., & Denora, N. (2020). Induced expression of P-gp and BCRP transporters on brain endothelial cells using transferrin functionalized nanostructured lipid carriers: A first step of a potential strategy for the treatment of Alzheimer's disease. *International Journal of Pharmaceutics*, *591*, 1-9. [120011]. https://doi.org/10.1016/j.ijpharm.2020.120011

Induced expression of P-gp and BCRP transporters on brain endothelial cells using transferrin functionalized nanostructured lipid carriers: A first step of a potential strategy for the treatment of Alzheimer's disease

Ilaria Arduino [a,1], Rosa Maria Iacobazzi [b,1], Chiara Riganti [c], Angela Assunta Lopedota [a], Maria Grazia Perrone [a], Antonio Lopalco [a], Annalisa Cutrignelli [a], Mariangela Cantore [d], Valentino Laquintana [a], Massimo Franco [a], Nicola Antonio Colabufo [a,e], Gert Luurtsema [f], Marialessandra Contino [a,*], Nunzio Denora [a,*]

[a] Department of Pharmacy - Pharmaceutical Sciences, University of Bari "Aldo Moro", Orabona St. 4, 70125 Bari, Italy
[b] Laboratory of Experimental Pharmacology, IRCCS Istituto Tumori "Giovanni Paolo II", O. Flacco St., 70124 Bari, Italy
[c] Department of Oncology, University of Torino, via Santena 5/bis, 10126 Torino, Italy
[d] Institute of Chemicals and Physical Process, CNR, Via E. Orabona, Bari, Italy
[e] Biofordrug s.r.l., Spin-off dell'Università degli Studi di Bari ALDO MORO, via Dante 99, 70019 Triggiano (Bari), Italy
[f] University of Groningen, University Medical Center Groningen, Department of Nuclear Medicine and Molecular Imaging, Hanzeplein 1, 9713 GZ Groningen, Netherlands

ABSTRACT

P-glycoprotein (P-gp) and Breast Cancer Resistance Protein (BCRP) are two transporters expressed in human neural stem/progenitor cells and at the Blood-Brain Barrier (BBB) level with decreased activity in the early stage of Alzheimer's disease (AD). Both proteins, have a protective role for the embryonic stem cells in the early developmental step, maintaining them in an undifferentiated state, and limit the access of exogenous and endogenous agents to the brain. Recently, MC111 selected from a P-gp/BCRP ligands library was investigated as multitarget strategy for AD treatment, considering its ability to induce the expression and activity of both proteins. However, MC111 clinical use could be limited for the ubiquitous physiological expression of efflux transporters and its moderate toxicity towards endothelial cells. Therefore, a selective MC111 delivery system based on nanostructured lipid carriers (NLC) functionalized with transferrin were developed. The results proved the formation of NLC with average size about 120 nm and high drug encapsulation efficiency (EE% greater than 50). In *vitro* studies on hCMEC/D3 cells revealed that the MC111 was selectively released by NLC at BBB level and then inducing the activity and expression of BCRP and P-gp, involved in the clearance of amyloid β peptide on brain endothelial cells.

1. Introduction

Alzheimer disease (AD) is a neurodegenerative illness representing the leading cause of dementia worldwide. It is estimated that about 35 million people over 60 years of age are affected by dementia and this number is expected to triplicate by 2050 (Prince et al., 2013). As known, the neuropathological features of AD are the presence of the senile plaques constituted by amyloid β peptide accumulation and the neurofibrillary tangles formed by highly phosphorylated *Tau* proteins (Contino et al., 2013; Kung, 2012). The current treatment is only aimed to hit the neuropsychiatric and behavioural symptoms using, as FDA approved AD therapy, cholinesterase inhibitors (tacrine, donepezil, rivastigmine, galantamine) and the *N*-methyl-D-aspartate receptor antagonist, memantine (Cummings et al., 2014). In this complex scenario, P-glycoprotein (P-gp) and Breast Cancer Resistance Protein (BCRP), two ATP-binding cassette (ABC) transporters proteins, play an important role in AD and might represent potential biomarkers for the development of new therapies. In fact, these two proteins highly expressed in human neural stem/progenitor cells and at the blood–brain barrier (BBB) level (Erdei et al., 2014; Islam et al., 2005), act as "protective barrier" for the

---

embryonic stem cells, maintaining them in an undifferentiated state. Endothelial cells at the BBB level produce soluble factors that in physiological conditions, being P-gp substrate, do not enter at the brain level as effluxed by the pump, while, in pathological condition as in AD, where the pump is downregulated, these factors are not effluxed and thus enter the BBB inducing a modification on the microenviroment and on the homeostasis of stem cells with a functional alteration in neurogenesis (Islam et al., 2005). Therefore, modulation of these ABC transporters could be suggested as a new strategy to promote cell self-renewal without differentiation. Moreover, P-gp exerts a pivotal role in the clearance of amyloid β peptide from the brain and thus, the decreased activity and expression of the transporter observed in AD is one of the causes of the senile plaque formation in the early stage of the disease (Colabufo et al., 2010; Contino et al., 2013; Deo et al., 2014). Considering the importance of P-gp and BCRP in the onset of AD, some of co-authors identified, from a P-gp/BCRP ligands library, compound MC111 as multitarget agent able to induce the expression and the activity of the two transporters exerting a neuroprotective anti-AD activity (Colabufo et al., 2018). However, this potential approach highlighted some limitations due to the ubiquitous physiological expression of the efflux transporters in different compartments of our body and to a moderate toxicity observed for endothelial cells. Therefore, to avoid side effects due to unspecific interactions, we designed a selective delivery system able to release MC111at the BBB, which integrity is usually preserved in neurodegenerative diseases, such as AD. Hence, brain targeting for the treatment of neurodegenerative diseases is still a challenge. Several approaches have been explored in order to allow brain delivery, and among these, the use of pharmaceutical nanoparticle systems seems to be one of the most promising strategies (Arduino et al., 2020; Lopalco et al., 2018a, 2018b; Laquintana et al., 2014). In particular, lipid-based nanosystems represent a promising strategy for the brain delivery due to their biocompatibility and inherent ability to reach the BBB even without any functionalization (Arduino et al., 2020; Tapeinos et al., 2017). In particular, nanostructured lipid carriers (NLCs) as a modified version of solid lipid nanoparticles (SLNs), represent an improved generation of this kind of nanoparticles. Indeed, the problems associated with SLNs such as a limited drug loading capacity and drug expulsion during storage are avoided by NLCs (Hsu et al., 2010). The lipid matrix in NLCs, which is composed of optimized solid and liquid lipids, could result in an imperfect crystal structure and therefore provide more room for drug accommodation, especially for hydrophobic drugs (Li et al., 2018). The efficacy of NLCs as BBB targeting can be further improved by coating their surface with ligands for specific receptors localized on the brain endothelial cells, such as transferrin receptors (TfR), which are highly expressed on the luminal side of brain capillary endothelial cells (Pinheiro et al., 2020; Lopalco et al., 2018a). Despite AD is accompanied by a BBB dysfunction, it was demonstrated that TfR levels are not altered by AD neuropathology and they do not significantly fluctuate with age (Bourassa et al., 2019). In this way, the lipid nanoparticles can benefit of an active drug targeting strategy towards BBB. The aim of this investigation was the development and characterization of Tf functionalized NLCs loaded with MC111, exploring its ability to be selectively delivered at BBB level, thus resulting as a promising approach for AD treatment. Accordingly, the NLCs were characterized for their size and size distribution, surface morphology, drug encapsulation efficiency and drug release profile. Moreover, the ability to target the BBB and to release the drug inside the cells as well as the activity of the new developed system on P-gp and BCRP, were studied on an *in vitro* BBB model (hCMEC/D3cells) in order to confirm the beneficial effect of the proposed strategy in comparison with the compound MC111 alone. This new targeting strategy can be considered innovative to hit the onset of AD, since the decreased expression/activity of P-gp and BCRP occurs at the first step of the disease. Therefore, this new approach could be the starting point of a new AD therapy, mainly in an early stage, for which to date a real cure is not available.

2. Materials and methods

2.1. Materials

All chemicals were of the highest purity available and were used as received without further purification or distillation. 1,2-distearoyl-*sn*-glycero-3-phosphoethanolamine-N-[carboxy(polyethylene glycol)-2000] (sodium salt) (DSPE-PEG(2000)-COOH) and1,2-distearoyl-*sn*-glycero-3-phosphoethanolamine-N-[poly(ethylene glycol)2000-*N'*-carboxyfluorescein] (ammonium salt) (18:0 PEG2000 PE CF) were purchased from Avanti Polar Lipids. Cetyl palmitate and oleic acid were purchased from Farmalabor. Pluronic F68, 1-ethyl-3-(3-dimethylamino-propyl) carbodiimide (EDC) and *N*-hydroxysuccinimide (NHS) were purchased from Sigma Aldrich. All solvents used were of analytical grade and purchased from Aldrich. All aqueous solutions were prepared using water obtained from a Milli-Q gradient A-10 system (Millipore, 18.2 MΩ·cm, organic carbon content $\geq$ 4 µg/L).

2.2. Preparation of nanostructured lipid nanoparticles loaded with MC111

NLCs loaded MC 111 with or without Tf –targeting moiety were prepared by an oil-in-water homogenization process at high temperature according to a procedure reported in literature (Arduino et al., 2020). Briefly, 1.5 mg of MC 111 was dissolved in 500 µL of hot methanol (65 °C) and, 80 mg of cetyl palmitate, 20 mg of oleic acid and 12 mg of DSPE-PEG (2000)-COOH were co-dissolved in chloroform (1 mL). Afterward, the methanol and chloroform solutions were softly stirred to obtain a homogeneous mixture, then this organic solution was added drop by drop to 5 mL of ultrapure water containing Pluronic F68 (1% p/v) at 65 °C and sonicated for 15 min by using a probe-tip ultrasonicator (0.27 W). The organic phase was quickly evaporated at 65 °C with a rotary evaporator. The aqueous solution was left at room temperature for 2 h to permit the complete evaporation of the organic solvents and, then, it was maintained at 4 °C for 15 min to allow the SLNs formation. To remove any surfactant, solvent residuals and non-encapsulated drug, the produced SLNs were carefully purified by using ultrapure water and centrifugal concentrators (CentriconCentriplus*YM100*) at 800 g for 1 h at 4 °C. Empty NLCs were made without the addition of MC111. To determine the cellular uptake of NLCs, the formulation contained a fluorescent PEG lipid. In particular, 40 µg of 18:0 PEG2000 PE CF was added to the organic phase before the sonication. All the nano-formulations were kept in ultrapure water at 4 °C.

2.3. Functionalization of nanostructured lipid nanoparticle with transferrin

The preparation of Tf functionalized NLCs was achieved by binding the carboxyl group of DSPE-PEG (2000)-COOH present on the surface of preformed NLCs, with the amino group of Tf as described in literature (Jhaveri et al., 2018). In order to activate the carboxylic group 4 mg of EDC and 1.5 mg of NHS (both are catalyst) were mixed in 1 mL of NLCs at 25 °C for 5 h, and immediately after, left under stirring at 4 °C for 8 h. Subsequently, 2 mg of Tf were added to activated NLCs and gently stirred at 4 °C for 24 h. The Tf-NLCs were purified by centrifugation under the same condition described above.

In order to investigate the density of Tf on the NLCs surface a Bicinchonic Acid assay (BCA) kit was adopted, evaluating, through indirect method, the percentage of unbound Tf compared to the total amount of Tf used for the conjugation. The absorbance at 540 nm was recorded (UV–vis spectroscopy) and the protein concentration was determined by comparison to a standard curve (5–0.2 mg/mL).

2.4. Evaluation of drug encapsulation efficiency

The encapsulation efficacy (EE %) values of MC111 loaded in hy-

drophobic core of NLCs were calculated by evaluating the drug content in 500 μL of the NLCs aqueous dispersion. In particular, NLCs were dissolved in 2 mL of hexane, in order to solubilize the lipid matrix, and 2 mL of DMSO for the extraction of MC111. The DMSO was analyzed for drug content by UV–vis spectroscopy (Perkin Elmer Lambda Bio20) exploiting the absorbance peak at 276 nm. MC111 concentration was estimated through calibration curve. The EE% values of drug were calculated according the following formula:

$$Encapsulation\ Efficacy\ (\%) = \frac{Weight\ of\ drug\ in\ NLCs}{Weight\ of\ drug\ added\ initially} \times 100$$

2.5. In vitro drug release study

Release studies of MC111 from NLCs were performed using Franz cells (Arduino et al., 2020), in particular the experiments were conducted in presence and absence of human serum in the donor compartment. Specifically, 300 μL of NLC-MC111 dispersion was diluted with 300 μL of water or human serum and placed on the diffusion barrier (area of 0.6 cm^2) formed by an artificial cellulose acetate membrane (0.1–0.5 kDa, Fisher Scientific Milano), which separates donor and receptor cells. Phosphate buffer (PBS, 10 mM, pH 7.4) was selected as receptor medium and it was continually stirred and maintained at a temperature of (37 ± 0.5) °C. In a total time of 96 h, 0.2 mL were collected from the receiving compartment at set times, and in order to maintain the sink conditions the same amount of fresh PBS was added in the receptor cell. The collected fractions were analyzed by UV/Vis to determine the drug content. Each experiment was performed in triplicate and was carried out in three independent Franz cells using three different batches of NLCs.

2.6. Particle size, size distribution and surface charge

The mean hydrodynamic diameter, size distribution, and ζ-potential values of the NLCs were determined by using the Zetasizer Nano ZS, Malvern Instruments Ltd., Worcestershire, UK. In particular, size and size distribution were measured by means of dynamic light scattering (DLS), at room temperature, after sample dilution in demineralized water. Size distribution was described in terms of polydispersity index (PDI) and the average particle size was reported as intensity mean diameter. The ζ-potential measurements were carried out by using a laser Doppler velocimetry (LDV), at room temperature, after sample dilution in freshly prepared aqueous KCl solution (1 mM). All reported data are presented as means ± standard deviation of three replicates.

2.7. Cells

hCMEC/D3 cells, a human brain microvascular endothelial stabilized cell line, were a kind gift from Prof. Pierre-Olivier Couraud (Institut Cochin, Centre National de la RechercheScientifique UMR 8104, INSERM U567, Paris, France) and were cultured according to (Weksler et al., 2013).

For cytotoxicity studies hCMEC/D3 cells, after coating the 96-well plate with 1% gelatin (SIGMA-G9391), were seeded at a density of 10,000 cells per well. For permeability experiments, cells were seeded at 50,000/cm^2 density and grown for 7 days up to confluence in 6-well Transwell devices (0.4 μm diameter pores-size, Transwell insert surface: 4.67 cm^2; Corning Life Sciences, Chorges, France for transport assays) or 24-well Transwell devices (0.4 μm diameter pores-size, Transwell insert surface: 0.33 cm^2; Corning Life Sciences for TEER measure), to allow the formation of a competent BBB. Before each experiment, TEER and permeability coefficients of 70 kDa-Dextran FITC, [^{14}C]-sucrose (589 mCi/mmol; PerkinElmer, Waltham, MA), [^{14}C]-inulin (10 mCi/mmol; PerkinElmer) and lucifer yellow (Invitrogen Life Technology, Milano, Italy), were measured as previously described (Monnaert et al., 2004; Riganti et al., 2014; Weksler et al., 2013) in BBB

cells in the absence of GB cells. TEER was measured using a Voltohmetro Millicell-ERS (Millipore, Billerica, MA), according to the manufacturer's instructions. The mean TEER value of the plastic insert in the absence of cells was 26.73 Ω cm^2 (n = 8). This value was subtracted from each value obtained in the presence of the cells.

2.8. Cytotoxicity assay

After 24 h necessary for the adhesion of hCMEC/D3 on 96 well gelatin coated plate, cells were treated for 24 h with NLC-MC111, Tf-NLC-MC111, empty NLCs and MC111 alone as a reference. The concentration range tested was 0.1–50 μM in terms of drug corresponding to a lipids concentration range of 5–3000 μg/mL. The results obtained were expressed in terms of % cell viability as a function of drug or lipids concentrations and represented with a histogram to be able to compare the toxicity of the drug as such and included in the NLCs and of empty nanovectors.

2.9. NLC uptake

hCMEC/D3 cells were seeded at 50,000/cm^2 density, and grown for 7 days up to confluence on sterile glass coverslips and incubated for 24 h with fluorescently labeled NLC (Fluo-NLC-MC111 and Fluo-Tf-NLC-MC111) at a final concentration of fluorophore of 10 μM, rinsed with PBS, fixed with 4% w/v paraformaldehyde for 15 min, washed three times with PBS and incubated with 4′,6-diamidino-2-phenylindole (DAPI, diluted 1:10,000, Sigma) for 3 min at room temperature in the dark. Cells were washed three times with PBS and once with water, then the slides were mounted with 4 μL of Gel Mount Aqueous Mounting and examined with a Leica DC100 fluorescence microscope (Leica Microsystems GmbH, Wetzlar, Germany). For each experimental point, a minimum of 5 microscopic fields were examined.

2.10. NLC permeability

hCMEC/D3 cells were seeded at 50,000/cm^2 density and grown for 7 days up to confluence in Transwell insert and incubated 24 h with NLC-MC111, functionalized Tf-NLC-MC111 and their fluorescently labeled counterparts at a final concentration of MC111of 10 μM. Cells were collected after gentle scraping, together with the medium of the upper and lower chamber. Cells were rinsed with 1 mL PBS, centrifuged at 1,200 g for 5 min and sonicated, then frozen at −20 °C and freeze-dried at 50 °C for 24 h and 0.060 mbar by using a *5 Lio Pascal DGT*. The lyophilized samples were treated with acetonitrile (500 μL) centrifuged (5000 rpm; 5 min). The supernatants were analyzed by HPLC (Zorbax Eclipse Plus C18; 60/40 = CH$_3$CN/H$_2$O, 1 mL/min; λ = 250 nm). Unknown concentrations of MC111 in samples obtained from NLC permeability experiment were determined by interpolation from a first order calibration curve (Y = mX + C; Y = peak area and X = drug concentration) built with known MC111 concentrations.

2.11. Immunoblot

Cells were rinsed with ice-cold lysis buffer (50 mM, Tris, 10 mM EDTA, 1% v/v Triton-X100), supplemented with the protease inhibitor cocktail set III (80 μM aprotinin, 5 mM bestatin, 1.5 mM leupeptin, 1 mM pepstatin; Calbiochem, San Diego, CA), 2 mM phenylmethylsulfonyl fluoride (PMSF) and 1 mM Na$_3$VO$_4$, then sonicated and centrifuged at 13,000g for 10 min at 4 °C. 20 μg of extracted proteins were subjected to SDS-PAGE and probed with the following antibodies: anti-Pgp (C219; Calbiochem), anti-BCRP (M-70; Santa Cruz Biotechnology Inc., Santa Cruz, CA), anti-β-tubulin (D-10 and TUJ1; Santa Cruz Biotechnology Inc.), followed by a peroxidase-conjugated secondary antibody (Bio-Rad Laboratories, Hercules, CA). The membranes were washed with Tris-buffered saline-Tween 0.1% v/v solution, and the proteins were detected by enhanced chemiluminescence (Bio-Rad Laboratories).

2.12. P-gp and BCRP activity

The ATPase activity was measured in membrane vesicles as described previously (Kopecka et al., 2014). After treatment for 24 h with NLC-MC111, functionalized Tf -NLC-MC111 and their empty counterparts, cells were washed with Ringer's solution (148.7 mM NaCl, 2.55 mM K_2HPO_4, 0.45 mM KH_2PO_4, 1.2 mM $MgSO_4$; pH 7.4), lysed on crushed ice with lysis buffer (10 mM Hepes/Tris, 5 mM EDTA, 5 mM EGTA, 2 mM dithiothreitol; pH 7.4) supplemented with 2 mM PMSF, 1 mM aprotinin, 10 μg/mL pepstatin, 10 μg/mL leupeptin, and subjected to nitrogen cavitation at 1200 psi for 20 min. Samples were centrifuged at $300 \times g$ for 10 min in the pre-centrifugation buffer (10 mMTris/HCl, 25 mM sucrose; pH 7.5), overlaid on a sucrose cushion (10 mMTris/HCl, 35% w/v sucrose, 1 mM EDTA; pH 7.5) and centrifuged at 14,000g for 10 min. The interface was collected, diluted in the centrifugation buffer (10 mM Tris/HCl, 250 mM sucrose; pH 7.5) and subjected to a third centrifugation at 100,000g for 45 min. The vesicle pellet was resuspended in 0.5 mL centrifugation buffer and stored at −80 °C until the use, after the quantification of the protein content. 100 μg of total proteins were immuno-precipitated with an anti-Pgp or ananti-BCRP antibody overnight at 4 °C using 25 μL of Pure Proteome A/G Mix Magnetic Beads (Millipore, Bedford, MA). 20 μg of the immuno-purified protein were incubated for 30 min at 37 °C with 50 μL of the reaction mix (25 mM Tris/HCl, 3 mM ATP, 50 mM KCl, 2.5 mM $MgSO_4$, 3 mM dithiothreitol, 0.5 mM EGTA, 2 mM ouabain, 3 mM NaN_3; pH 7.0). The reaction was stopped by adding 0.2 mL ice-cold stopping buffer (0.2% w/v ammonium molybdate, 1.3% v/v H_2SO_4, 0.9% w/v SDS, 2.3% w/v trichloroacetic acid, 1% w/v ascorbic acid). After 30 min incubation at room temperature, the absorbance of the phosphate hydrolysed from ATP was measured at 620 nm, using a Packard EL340 microplate reader (Bio-Tek Instruments). The absorbance was converted into nmoles hydrolysed phosphate (Pi)/min/mg proteins, according to the titration curve previously prepared.

2.13. Statistical analysis

Results were analysed by a one-way analysis of variance (ANOVA) and Tukey's test, using GraphPad Prism software (v 6.01). $p < 0.05$ was considered significant. All data were expressed as means ± SD. For cytotoxicity assay a two-way analysis of variance (ANOVA) followed by the Bonferroni post hoc tests (GraphPad Prism vers. 5.0) was used and * $p < 0.05$, ** $p < 0.01$, *** $p < 0.001$ were considered significant.

3. Results and discussion

3.1. Preparation and characterization of nanostructured lipid carrier loaded MC111

In the present work the NLCs have been developed as a valid alternative to the SLNs. Despite SLNs offered many advantages in the delivery of drugs and had impressive results in antitumor therapy, they face the problems of low drug encapsulation and increased drug expulsion during storage (Han et al., 2014). For these reasons, NLCs were developed to overcome the drawbacks of SLNs. In order to obtain a

drug delivery system for MC111, NLCs containing MC111 and functionalized with Tf were prepared by hot homogenization technique as described in literature (Arduino et al., 2020). The NLCs were also prepared using a PEG modified phospholipid, which allowed the binding with Tf by its carboxylic group, but also the function of reducing the opsonization of NLCs and the uptake by the endothelial reticular system (Saraiva et al., 2016). In particular, Tf was conjugated to the carboxyl group of DSPE-PEG (2000)-COOH as already described before (Jhaveri et al., 2018). Moreover, for cellular studies, fluorescent NLCs were prepared by adding a fluorescent lipid to the preparation. Then, the fully characterization in terms of dimension, PDI, ζ-potential, EE% and Tf coupling efficiency was carried out. Results are summarized in Table 1.

As reported in Table 1, the particle size of the empty NLCs, Tf-NLC, NLC-MC111, Tf-NLC-MC111, fluorescent NLC-MC111 and fluorescent Tf-NLC-MC111 were found to be approximately around 120 nm with narrow distribution range, which was reflected by their small polydispersity index (<0.2). Particle size < 150 nm is an advantage for NLCs because it decreases uptake by the liver, prolongs circulation time in the blood, and improves bioavailability. Small vectors are also minimally phagocytosed by macrophages, so destruction and clearance are minimized (Li et al., 2018). In addition to particle size, the surface ζ-Potential also plays an important role in determining the in vivo fate of nanoparticles. The ζ-Potential measurements highlighted the presence of an overall negative charge on the surface of all NLCs and provided values ranging from −31.7 to 42.7 mV that indicated their good colloidal stability in aqueous solution and a favourable fate in the blood stream (Table 1). (Li et al., 2018). In fact, nanoparticles with neutral and negative charges have been demonstrated to reduce the adsorption of serum proteins in the blood stream, which are also negatively charged, thus resulting in longer circulation respect to the positively charged nanoparticles (Alexis et al., 2008; Tsou et al., 2017). Moreover, it has been shown that nanoparticles with high positive charge cause immediate toxicity to the BBB (Lockman et al., 2004; Saraiva et al., 2016).

For all the NLCs, the EE % values represent the amount (w/w %) of the drug incorporated in the lipid core of NLCs with respect to the starting drug amount employed for the preparation of lipid nanovectors. The EE values were 56.2 ± 1.2% and 58.3 ± 2.3% for NLC-MC111 and Tf-NLC-MC111 respectively (Table 1), they did not exhibit any significant alteration after Tf decoration, indicating that the stability of the NLCs was not influenced by Tf (Pinheiro et al., 2020). Fluorescent NLCs showed a small reduction in EE% values, in particular 49.7 ± 3.7% and 50.1 ± 1.8% for Fluo-NLC-MC111 and Fluo-Tf-NLC-MC111 respectively (Table 1). Nevertheless, values approximately equal to and greater than 50% revealed good encapsulation efficiency (Saraiva et al., 2016).

In addition, the amount of Tf in all functionalized NLCs was quantified via BCA assay, and the results showed that the binding efficiency of Tf was 61.5 ± 3.2% and 61.1 ± 2.6% for Tf-NLC and Tf-NLC-MC111 respectively, and 70.7 ± 1.4 for fluorescent Tf-NLC-MC111 (Table 1). The functionalization of NLCs with Tf improved the delivery of MC111 to BBB by internalization in endothelial cells by means of Tf-receptor mediated endocytosis.

In vitro drug release study was performed on NLC-MC111 and Tf-NLC-MC111 using Franz-diffusion cells at 37 °C in PBS (pH 7.4). As reported in literature, drug release from lipid-based nanoparticles

Table 1

Intensity-average hydrodynamic diameter and corresponding polydispersity index (PDI) determined by DLS, ζ-Potential value, drug encapsulation efficiency (EE%) and conjugated Tf % of all prepared NLCs.

Nanoformulation	d_{mean} (nm)	PolyDispersity Index (PDI)	ζ-potential (mV)	Encapsulation Efficiency (EE%)	Conjugated Tf (%)
Empty NLC	137.8 ± 2.4	0.155 ± 0.022	−42.7 ± 0.9	/	/
NLC-MC111	117.4 ± 2.1	0.200 ± 0.028	−41.2 ± 0.8	56.2 ± 1.2	/
Tf-NLC	128.4 ± 1.0	0.170 ± 0.033	−41.8 ± 0.6	/	61.5 ± 3.2
Tf-NLC-MC111	118.4 ± 2.1	0.202 ± 0.028	−38.6 ± 0.9	58.3 ± 2.3	61.1 ± 2.6
Fluo-NLC-MC111	126.7 ± 1.9	0.189 ± 0.025	−39.4 ± 0.6	49.7 ± 3.7	/
Fluo-Tf-NLC-MC111	119.6 ± 1.1	0.177 ± 0.033	−31.7 ± 1.0	50.1 ± 1.8	70.7 ± 1.4

Mean ± SD are reported, n = 3.

occurs following the degradation of the lipid matrix of nanoparticles by the enzymes present in cells (Arduino et al., 2020). For this reason, the experiments were conducted in presence and absence of human serum in the donor compartment. It was clearly possible to observe that in absence of human serum no release of MC111 occurred for both formulations (Fig. 1), while in presence of human serum the percentage of MC111 released from NLCs was found to be 95.9% for unfunctionalized NLCs (NLC-MC111) and 87.9% for functionalized NLCs (Tf-NLC-MC111) in 96 h of incubation (Fig. 1). Noteworthy, the coating of Tf on the surface of NLCs led to much slower release of the drug in comparison to unfunctionalized NLCs and this behaviour is quite in agreement with data found in literature (Lopalco et al., 2018a; Sonali et al., 2016).

3.2. Cytotoxicity study

The effect on hCMEC/D3 cells viability induced by empty NLCs, NLC-MC111, its functionalized counterpart Tf-NLC-MC11 and free MC111 after 24 h of treatment, was determined by the MTT assay (Fanizza et al., 2016; Iacobazzi et al., 2017; Depalo et al., 2017). As can be seen from the graph in Fig. 2, the exposure of cells to MC111 alone revealed a drug induced toxicity higher than that observed in cells treated with NLC-MC111, at each tested concentration. In particular, starting from concentration 10 μM in terms of MC111 (corresponding to a 600 μg/mL concentration of lipids) up to 0.1 μM (corresponding to a 6 μg/mL concentration of lipids) the % cell viability values recorded for cells treated with MC111-encapsulated in NLC, both Tf-functionalized or not, were significantly higher than values obtained for free MC111-treated cells. Such a result can be positively considered for the purpose to overcome one of the limits of the clinical use of MC111, namely its toxicity towards endothelial cells. The MTT assay was also useful for selecting the concentration 10 μM in terms of MC111 as the most appropriate to perform the permeability test with NLC-MC111, Tf-functionalized or not, and with free MC111, balancing the cytotoxic effects on endothelial cells and the limit of instrumental detection of MC111. Namely, at concentration 10 μM, the % cell viability values were $38 \pm 1\%$, $66 \pm 4\%$, $60 \pm 3\%$ for MC111, NLC-MC111 and Tf-NLC-MC111, respectively. Noteworthy, Tf-NLC-MC111 showed a slightly higher cytotoxicity respect to NLC-MC11 in the same concentration range, probably because the targeting moiety, giving to the system the ability to be internalized via Tf-receptor-mediated endocytosis, allows a

greater intracellular drug accumulation. Another aspect to be considered, not least in importance, is that empty NLC, *per sè,* showed no considerable toxicity towards endothelial cells at each tested concentration expressed in terms of lipids.

3.3. Uptake and permeability of nanostructured lipid carrier loaded MC111 at blood-brain barrier level

The ABC transporters, mainly Pgp and BCRP, expressed on BBB are the primary intended targets of NLC-loaded MC111. We thus set up the biological assays in hCMEC/D3 cells, cultured in BBB-forming conditions (Weksler et al., 2013). The mean permeability to 70-kDa dextran, sucrose and inulin, considered as indexes of a competent BBB (Monnaert et al., 2004), were: $0.23 \pm 0.06 \times 10^{-3}$ cm min^{-1}, $0.98 \pm 0.25 \times 10^{-3}$ cm min^{-1}, $0.38 \pm 0.09 \times 10^{-3}$ cm min^{-1}, respectively. The mean TEER value was 34 ± 6 Ω cm^2. Overall, these values suggested a competent BBB. First, we aimed at clarifying if NLC were internalized by BBB endothelial cells and showed a good transcellular permeability. To investigate the first point, we incubated hCMEC/D3 cells with Fluo-NLC-MC111 and Fluo-Tf-NLC-MC111 to track their intracellular localization. As shown in Fig. 3, after 24 h both Fluo-NLC-MC111 and Fluo-Tf-NLC-MC111were detected in the cytosol of hCMEC/D3 cells. The distribution was homogeneous for Fluo-NLC-MC111 (Fig. 3, upper panel), while Fluo-Tf-NLC-MC111 produced a stronger and more clusterized fluorescence pattern (Fig. 3, lower panel). These punctuate fluorescence spots are indicative of the interaction of Fluo-Tf-NLC-MC111 with the surface TfR and/or of a temporary accumulation within endosomes after the TfR-triggered endocytosis (Fig. 3, lower panel). The receptor-mediated endocytosis has been already reported for Tf-conjugated peptides (Crook et al., 2020) and nanoparticles (dos Santos Rodrigues et al., 2020; Li et al., 2016; Sahin et al., 2017) that enter the BBB cells and are delivered to CNS parenchyma following this pathway of transcytosis (Choudhury et al., 2018; Tashima, 2020).

After the intracellular uptake, we next investigated if the NLCs can cross the BBB and reach the baso-lateral compartment of BBB inducing the release of the active small molecule MC111, through permeability experiments.

Permeation experiments through hCMEC/D3 cells monolayer were performed by using concentration of drug loaded in NLCs of 10 μM. The ability of NLC-MC111, Tf-NLC-MC111, Fluo-NLC-MC111 and Fluo-Tf-
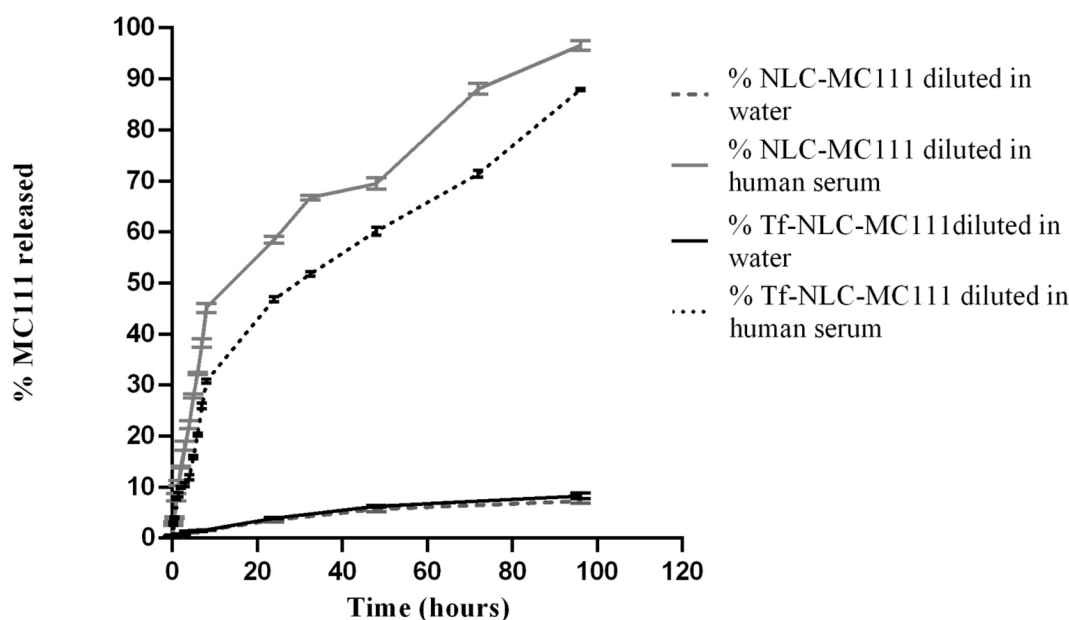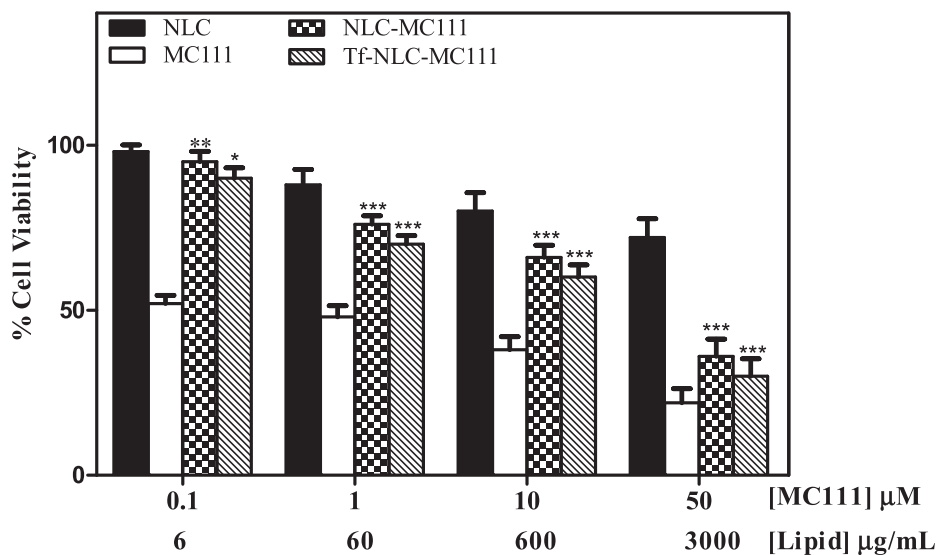

Fig. 1. In vitro release profiles of MC111 from NLCs functionalized (Tf-NLC-MC111) and unfunctionalized (NLC-MC111) in PBS at 37 °C. NLCs were diluted with water or human serum in the donor compartment. Mean ± SD are reported, n = 3.

Fig. 2. Cell viability of hCMEC/D3 cells after treatment for 24 h with MC111, NLC-MC111, Tf-NLC-MC111 and empty NLC (0.1–50 μM in terms of drug concentration and 6–3000 μg/mL in terms of surfactant). Each compound was tested in triplicate, and the experiments were repeated three times. Statistical significance was calculated using a two-way analysis of variance (ANOVA) followed by the Bonferroni post hoc tests (GraphPad Prism vers. 5) and referred to free MC111. * $p < 0.05$, ** $p < 0.01$, *** $p < 0.001$.
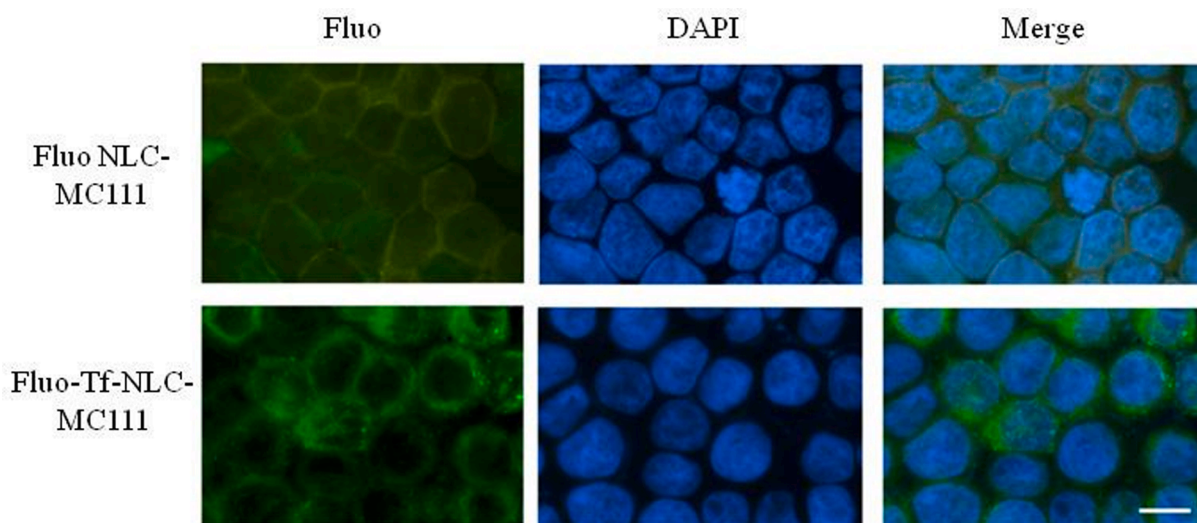
Fig. 3. Intracellular uptake of fluorescently-labelled NLC-MC111, either non functionalized (Fluo NLC-MC111) or functionalized (Tf-Fluo-NLC-MC111), incubated 24 h in the culture medium of hCMEC/D3 cells at a final concentration of fluorophore of 10 μM. Nuclei were counterstained with DAPI. Cells were analyzed by fluorescence microscope (objective: 63 x; ocular lens: 10 x). The image is representative of 1 out of 3 independent experiments. Bar: 10 μm.

NLC-MC111 to cross the in vitro BBB model was assessed at 24 h by measuring the concentration of MC111 in the upper, cellular and lower compartments. By measuring MC111 in the samples obtained from the permeability experiment, it was clear that when MC111 was loaded in the NLC (NLC-MC111) it divided among the three compartments, upper, cellular and lower, with a percentage of $49 \pm 4\%$, $43 \pm 2\%$ and $8 \pm 2\%$, respectively. Functionalizing NLC with transferrin (Tf-NLC-MC111), MC111 did not pass into the lower compartment but it accumulated in cells ($63 \pm 3\%$) and the remaining amount ($37 \pm 3\%$), was detected in the upper compartment. The transferrin effect is also confirmed when fluorescent NLCs (Fluo-NLC-MC111) have been prepared. In this case MC111 is divided between $42 \pm 3\%$, $46 \pm 1\%$ and $10 \pm 2\%$ in the upper, cellular and lower compartment, respectively while in the presence of transferrin (Fluo-Tf-NLC-MC111) MC111 was not found in the lower compartment but only in the upper one and in the cells with a percentage of $48 \pm 5\%$ and $51 \pm 5\%$, respectively (Fig. 4).

In the experimental conditions used, the rate of paracellular leakage of substrates was very low, as measured experimentally in this work and in agreement with previous studies on hCMEC/D3 cells (Riganti et al.,

2014; Salaroglio et al., 2019, 2018; Weksler et al., 2013). According to permeability coefficient data, to the fluorescence pattern and to the distribution of MC111, we reasonably believe that the functionalization with Tf could strongly restricts the delivery of NLC-MC111 to the CNS compartment. Moreover, by increasing the concentration of the compound entrapped within the BBB cells or facing the luminal face of BBB, this innovative drug delivery system could increase the possibility of MC111 to interact with proteins expressed on the luminal side of BBB, such as P-gp and BCRP.

3.4. Effects of nanostructured lipid carrier loaded MC111 on P-gp and BCRP

We previously observed that MC111 increases the amount of and activity of P-gp and BCRP in breast cancer and colon cancer cells (Colabufo et al., 2018). Thus, we investigated the effect of NLCs on these transporters on BBB. P-gp and BCRP proteins, which were constitutively present in hCMEC/D3 cells (Riganti et al., 2014; Weksler et al., 2013), resulted unmodified by empty NLC, both with and without Tf. Notably,
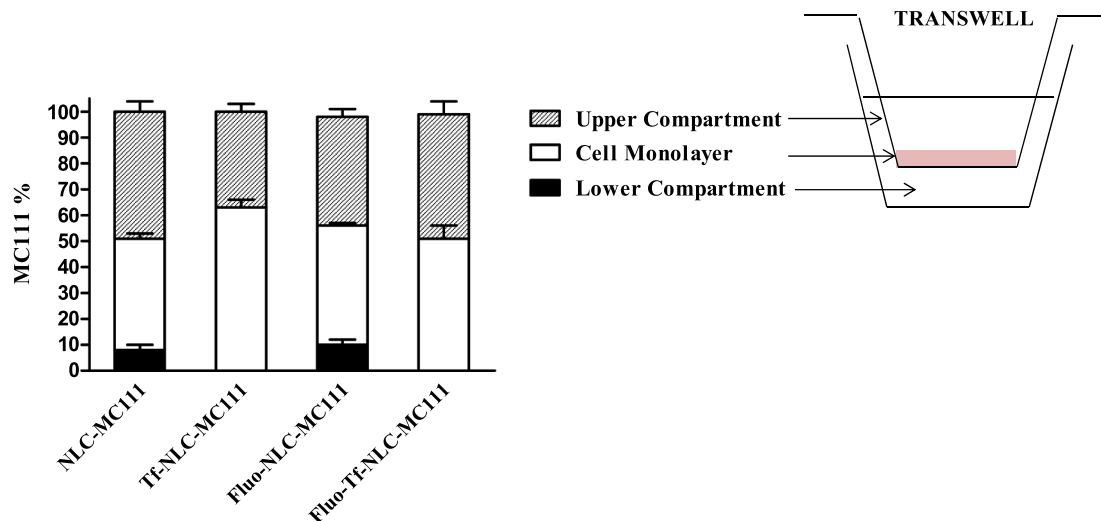
Fig. 4. Percentage of MC111 detected on upper, lower and cellular compartments along with the graphical sketch of the transwell insert used for the permeability assay performed incubating hCMEC/D3 cells for 24 h with NLC-MC111, functionalized Tf-NLC-MC111 and their fluorescently labeled counterparts.

NLC-MC111, in particular if conjugated with Tf, increased the expression of both proteins (Fig. 5A). Such increase was paralleled by a similar change in the transporters' activity, namely, empty NLC did not modify neither P-gp nor BCRP activity, which was instead augmented by NLC-MC111. The increase was maximal in cells treated with Tf-NLC-MC111 (Fig. 5B–C). This trend suggested that MC111 was responsible for the increase in P-gp and BCRP amount, thus explaining the higher activity of the transporters. Tf-conjugated NLCs were the most effective formulations, likely because they delivered a higher amount of MC111 inside the cells, resulting in an increased amount of the transporters. This can be due to increased transcription and/or stability of P-gp and BCRP. Higher was the protein level, higher was the ATPase activity, an index of the maximal catalytic efficiency of the proteins.

P-gp is heavily involved in the clearance of amyloid β peptide from brain parenchima (Miller et al., 2008) and the decrease in P-gp in brain microvascular endothelial cells has been identified as one of the early sign of AD (Hartz et al., 2016; Park et al., 2014; Rosas-Hernandez et al., 2020). Therein, preserving or even increasing the activity of P-gp on BBB cells may be regarded as a promising strategy in preventing the neurological damage due to the accumulation of amyloid β peptide. The role of BCRP in AD is controversial. The protein was not found downregulated in classical AD, but only in the so-called severe capillary cerebral amyloid angiopathy (Carrano et al., 2014). Pharmacological inhibition of

BCRP indicated that it is also involved in the baso-apical efflux of amyloid β peptide (Shubbar and Penny, 2020). Hence, increasing at the same time P-gp and BCRP activity, as MC111 does, may be a successful strategy in promoting the clearance of amyloid β peptide from brain.

P-gp and BCRP are the main ABC transporters present in adult BBB (Verscheijden et al., 2020). Species-related studies indicated that P-gp is abundantly expressed in rodents, while BCRP plays a predominant role in humans in effluxing catabolites, xenobiotics and drugs (Warren et al., 2009). These observations are in line with our findings, reporting a higher basal activity of BCRP than of P-gp in human hCMEC/D3 cells. The expression analysis of P-gp and BCRP in $mdr1^{-/-}$ and $bcrp^{-/-}$ mice pointed out a possible reciprocal regulation between the transporters, meaning that when one protein is down-regulated the other one shows a compensatory up-regulation, and *vice-versa* (Cisternino et al., 2004). Since MC111 increased P-gp expression, the risk of a simultaneous down-regulation of BCRP, with a consequent reduction in the clearance of β-amyloid, xenobiotics and drugs from CNS parenchima, could not be excluded *a priori*, but our assays demonstrate that MC111 was able to increase both P-gp and BCRP at the same time. This feature avoids a dangerous alteration in the CNS homeostasis due to the decrease expression or activity of solely P-gp or BCRP.
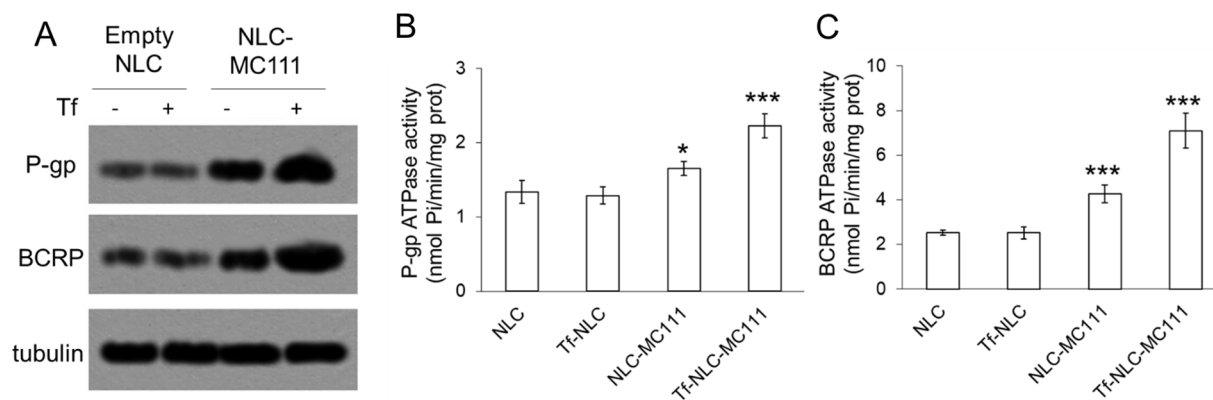

Fig. 5. hCMEC/D3 cells were treated 24 h with MC111-loaded NLC, 10 μM in terms of drug or with empty NLCs at concentration normalized using drug-loaded NLCs as a reference, with (+) or without (−) Tf. A. Immunoblot of the indicated proteins. Tubulin was used as control of equal protein loading. The image is representative of 1 out of 3 experiments with similar results. B-C. Spectrophotometric measurement of P-gp and BCRP activity, performed in triplicate. Data are means + SD (n = 3). *p < 0.05, ***p < 0.001: NLC-MC111/Tf-NLC-MC111 vs empty NLC (NLC).

4. Conclusions

We identified as new anti-AD therapeutic approach the small molecule MC111 that was active as inducer of the expression and activity of the two transporters, P-gp and BCRP, which result "inactivated" in the early stage of the pathology. The promising results found with this new "regenerative" approach has some limitation due to the physiological expression of both transporters in different compartments of our body and to the MC111 toxicity observed at the endothelial cells level. For these reasons, with the aim to overcome the limits of MC111, we adopted a site-targeted strategy by the design of a novel drug delivery system, namely NLCs functionalized with transferrin, able to directly release MC111 to the brain endothelial cells by the use of transferrin as targeting moiety, limiting side-effects. The targeting strategy allows MC111 to selectively induce in vitro the expression of P-gp and BCRP transporters on brain endothelial cells and thus triggering the clearance of amyloid β peptide from the brain. To date, only symptomatic therapies are used for the treatment of AD. This work represents an innovative approach because the MC111 molecule impacts on the first stage of the disease and not on its symptoms.

CRediT authorship contribution statement

Ilaria Arduino: Methodology, Writing - original draft, Writing - review & editing. **Rosa Maria Iacobazzi:** Methodology, Validation, Writing - original draft. **Chiara Riganti:** Methodology, Validation. **Angela Assunta Lopedota:** Formal analysis, Validation. **Maria Grazia Perrone:** Formal analysis, Validation. **Antonio Lopalco:** Resources. **Annalisa Cutrignelli:** Investigation. **Mariangela Cantore:** Investigation. **Valentino Laquintana:** Formal analysis, Validation. **Massimo Franco:** Data curation. **Nicola Antonio Colabufo:** Investigation, Writing - review & editing. **Gert Luurtsema:** Supervision. **Marialessandra Contino:** Writing - review & editing, Supervision, Project administration. **Nunzio Denora:** Writing - review & editing, Supervision, Project administration.

Declaration of Competing Interest

The authors declare that they have no known competing financial interests or personal relationships that could have appeared to influence the work reported in this paper.

Acknowledgements

References

Alexis, F., Pridgen, E., Molnar, L.K., Farokhzad, O.C., 2008. Factors affecting the clearance and biodistribution of polymeric nanoparticles. Mol. Pharm. 5, 505–515.

Arduino, I., Depalo, N., Re, F., Dal Magro, R., Panniello, A., Margiotta, N., Fanizza, E., Lopalco, A., Laquintana, V., Cutrignelli, A., Lopedota, A.A., Franco, M., Denora, N., 2020. PEGylated solid lipid nanoparticles for brain delivery of lipophilic kiteplatin Pt (IV) prodrugs: An in vitro study. Int. J. Pharm. 583, 119351.

Bourassa, P., Alata, W., Tremblay, C., Paris-Robidas, S., Calon, F., 2019. Transferrin receptor-mediated uptake at the blood-brain barrier is not impaired by Alzheimer's disease neuropathology. Mol. Pharm. 16, 583–594.

Carrano, A., Snkhchyan, H., Kooij, G., van der Pol, S., van Horssen, J., Veerhuis, R., Hoozemans, J., Rozemuller, A., de Vries, H.E., 2014. ATP-binding cassette transporters P-glycoprotein and breast cancer related protein are reduced in capillary cerebral amyloid angiopathy. Neurobiol. Aging 35, 565–575.

Choudhury, H., Pandey, M., Chin, P.X., Phang, Y.L., Cheah, J.Y., Ooi, S.C., Mak, K.K., Pichika, M.R., Kesharwani, P., Hussain, Z., Gorain, B., 2018. Transferrin receptors-targeting nanocarriers for efficient targeted delivery and transcytosis of drugs into the brain tumors: a review of recent advancements and emerging trends. Drug Deliv. Transl. Res. 8, 1545–1563.

Cisternino, S., Mercier, C., Bourasset, F., Roux, F., Scherrmann, J.M., 2004. Expression, up-regulation, and transport activity of the multidrug-resistance protein Abcg2 at the mouse blood-brain barrier. Cancer Res 64, 3296–3301.

Colabufo, N.A., Berardi, F., Cantore, M., Contino, M., Inglese, C., Niso, M., Perrone, R., 2010. Perspectives of P-glycoprotein modulating agents in oncology and neurodegenerative diseases: pharmaceutical, biological, and diagnostic potentials. J. Medicinal Chem. 53, 1883–1897.

Colabufo, N.A., Contino, M., Cantore, M., Berardi, F., Perrone, R., Tonazzi, A., Console, L., Panaro, M.A., Savolainen, H., Luurtsema, G., 2018. An innovative small molecule for promoting neuroreparative strategies. RSC Adv. 8, 5451–5458.

Contino, M., Cantore, M., Leopoldo, M., Colabufo, N., 2013. Biomarkers for the early diagnosis of Alzheimer's disease: The challenge of XXI century. Adv. Alzheimer's Disease 02, 13–30.

Crook, Z.R., Girard, E., Sevilla, G.P., Merrill, M., Friend, D., Rupert, P.B., Pakiam, F., Nguyen, E., Yin, C., Ruff, R.O., Hopping, G., Strand, A.D., Finton, K.A.K., Coxon, M., Mhyre, A.J., Strong, R.K., Olson, J.M., 2020. A TfR-binding cystine-dense peptide promotes blood-brain barrier penetration of bioactive molecules. J. Mol. Biol. 432, 3989–4009.

Cummings, J.L., Morstorf, T., Zhong, K., 2014. Alzheimer's disease drug-development pipeline: few candidates, frequent failures. Alzheimer's Res. Therapy 6, 37–37.

Deo, Anand K., Borson, Soo, Link, Jeanne M., Domino, Karen, Eary, Janet F., Ke, Ban, Richards, Todd L., Mankoff, David A., Minoshima, Satoshi, O'Sullivan, Finbarr, Eyal, Sara, Hsiao, Peng, Maravilla, Ken, Unadkat, Jashvant D., 2014. Activity of P-glycoprotein, a β-amyloid transporter at the blood-brain barrier, is compromised in patients with mild Alzheimer disease. J. Nucl. Med.: Off. Publ., Soc. Nucl. Med. 55, 1106–1111.

Depalo, Nicoletta, Iacobazzi, Rosa, Valente, Gianpiero, Arduino, Ilaria, Villa, Silvia, Canepa, Fabio, Laquintana, Valentino, Fanizza, Elisabetta, Striccoli, Marinella, Annalisa, Cutrignelli, Lopedota, Angela, Porcelli, Letizia, Azzariti, Amalia, Franco, Massimo, Curri, Maria, Denora, Nunzio, 2017. Sorafenib delivery nanoplatform based on superparamagnetic iron oxide nanoparticles magnetically targets hepatocellular carcinoma. Nano Res., 10.

dos Santos, Rodrigues, Sanjay Arora, Bruna, Kanekiyo, Takahisa, Singh, Jagdish, 2020. Efficient neuronal targeting and transfection using RVG and transferrin-conjugated liposomes. Brain Res. 1734, 146738.

Erdei, Zsuzsa, Lorincz, Reka, Szebenyi, Kornelia, Péntek, Adrienn, Varga, Nóra, Liko, Istvan, Várady, György, Szakács, Gergely, Orbán, Tamás, Sarkadi, Balázs, Apati, Agota, 2014. Expression pattern of the human ABC transporters in pluripotent embryonic stem cells and in their derivatives. Cytometry. Part B, Clin. Cytometry 86.

Fanizza, Elisabetta, Urso, Carmine, Iacobazzi, Rosa, Depalo, Nicoletta, Corricelli, Michela, Panniello, Annamaria, Agostiano, Angela, Denora, Nunzio, Laquintana, Valentino, Striccoli, Marinella, Curri, M., 2016. Fabrication of photoactive heterostructures based on quantum dots decorated with Au nanoparticles. Sci. Technol. Adv. Mater. 17, 98–108.

Han, Yiqun, Zhang, Ying, Li, Danni, Chen, Yuanyuan, Sun, Jiping, Kong, Fansheng, 2014. Transferrin-modified nanostructured lipid carriers as multifunctional nanomedicine for codelivery of DNA and doxorubicin. Int. J. Nanomed. 9, 4107–4116.

Hartz, Anika M.S., Zhong, Yu, Wolf, Andrea, LeVine, Harry, 3rd, Miller, David S., Bauer, Björn, 2016. Aβ40 reduces P-glycoprotein at the blood-brain barrier through the ubiquitin-proteasome pathway. J. Neurosci.: Off. J. Soc. Neurosci. 36, 1930–1941.

Hsu, S.H., Wen, C.J., Al-Suwayeh, S.A., Chang, H.W., Yen, T.C., Fang, J.Y., 2010. Physicochemical characterization and in vivo bioluminescence imaging of nanostructured lipid carriers for targeting the brain: apomorphine as a model drug. Nanotechnology 21, 405101.

Iacobazzi, R.M., Porcelli, L., Lopedota, A.A., Laquintana, V., Lopalco, A., Cutrignelli, A., Altamura, E., Di Fonte, R., Azzariti, A., Franco, M., Denora, N., 2017. Targeting human liver cancer cells with lactobionic acid-G(4)-PAMAM-FITC sorafenib loaded dendrimers. Int. J. Pharm. 528, 485–497.

Islam, M.O., Kanemura, Y., Tajria, J., Mori, H., Kobayashi, S., Shofuda, T., Miyake, J., Hara, M., Yamasaki, M., Okano, H., 2005. Characterization of ABC transporter ABCB1 expressed in human neural stem/progenitor cells. FEBS Lett 579, 3473–3480.

Jhaveri, Aditi, Deshpande, Pranali, Pattni, Bhushan, Torchilin, Vladimir, 2018. Transferrin-targeted, resveratrol-loaded liposomes for the treatment of glioblastoma. J. Control. Release 277, 89–101.

Kopecka, Joanna, Salzano, Giuseppina, Campia, Ivana, Lusa, Sara, Ghigo, Dario, De Rosa, Giuseppe, Riganti, Chiara, 2014. Insights in the chemical components of liposomes responsible for P-glycoprotein inhibition. Nanomed.: Nanotechnol. Biol. Med. 10, 77–87.

Kung, Hank F., 2012. The β-amyloid hypothesis in Alzheimer's disease: seeing is believing. ACS Med. Chem. Lett. 3, 265–267.

Laquintana, Valentino, Denora, Nunzio, Lopalco, Antonio, Lopedota, Angela, Cutrignelli, Annalisa, Lasorsa, Francesco Massimo, Agostino, Giulia, Franco, Massimo, 2014. Translocator protein ligand–PLGA conjugated nanoparticles for 5-fluorouracil delivery to glioma cancer cells. Mol. Pharm. 11, 859–871.

Li, Shanghao, Amat, Daniel, Peng, Zhili, Vanni, Steven, Raskin, Scott, De Angulo, Guillermo, Othman, Abdelhameed M., Graham, Regina M., Leblanc, Roger M., 2016. Transferrin conjugated nontoxic carbon dots for doxorubicin delivery to target pediatric brain tumor cells. Nanoscale 8, 16662–16669.

Li, Xin, Jia, Xiaoqian, Hu, Niu, 2018. Nanostructured lipid carriers co-delivering lapachone and doxorubicin for overcoming multidrug resistance in breast cancer therapy. Int. J. Nanomed. 13, 4107–4119.

Lockman, Paul R., Koziara, Joanna M., Mumper, Russell J., Allen, David D., 2004. Nanoparticle surface charges alter blood-brain barrier integrity and permeability. J. Drug Target. 12, 635–641.

Lopalco, Antonio, Annalisa, Cutrignelli, Denora, Nunzio, Lopedota, Angela, Franco, Massimo, Laquintana, Valentino, 2018a. Transferrin functionalized liposomes loading dopamine HCl: development and permeability studies across an in vitro model of human blood-brain barrier. Nanomaterials 8, 178.

Lopalco, Antonio, Cutrignelli, Annalisa, Denora, Nunzio, Perrone, Mara, Iacobazzi, Rosa, Fanizza, Elisabetta, Lopedota, Angela, Depalo, Nicoletta, de Candia, Modesto, Franco, Massimo, Laquintana, Valentino, 2018b. Delivery of proapoptotic agents in glioma cell lines by TSPO ligand-dextran nanogels. Int. J. Mol. Sci. 19, 1155.

Miller, David S., Bauer, Björn, Hartz, Anika M.S., 2008. Modulation of P-glycoprotein at the blood-brain barrier: opportunities to improve central nervous system pharmacotherapy. Pharmacol. Rev. 60, 196–209.

Monnaert, V., Tilloy, Sebastien, Bricout, H., Fenart, Laurence, Cecchelli, Romeo, Monflier, Eric, 2004. Behavior of alpha-, beta-, and gamma-cyclodextrins and their derivatives on an in vitro model of blood-brain barrier. J. Pharmacol. Exp. Therapeutics 310, 745–751.

Park, R., Kook, S.Y., Park, J.C., Mook-Jung, I., 2014. Aβ1-42 reduces P-glycoprotein in the blood-brain barrier through RAGE-NF-κB signaling. Cell Death Dis. 5, e1299.

Pinheiro, R.G.R., Granja, A., Loureiro, J.A., Pereira, M.C., Pinheiro, M., Neves, A.R., Reis, S., 2020. Quercetin lipid nanoparticles functionalized with transferrin for Alzheimer's disease. Eur. J. Pharm. Sci. 148, 105314.

Prince, M., Bryce, R., Albanese, E., Wimo, A., Ribeiro, W., Ferri, C.P., 2013. The global prevalence of dementia: a systematic review and metaanalysis. Alzheimers Dement 9, 63–75.e2.

Riganti, C., Salaroglio, I.C., Pinzòn-Daza, M.L., Caldera, V., Campia, I., Kopecka, J., Mellai, M., Annovazzi, L., Couraud, P.-O., Bosia, A., Ghigo, D., Schiffer, D., 2014. Temozolomide down-regulates P-glycoprotein in human blood-brain barrier cells by disrupting Wnt3 signaling. Cell Mol. Life Sci. 71, 499–516.

Rosas-Hernandez, Hector, Cuevas, Elvis, Raymick, James B., Robinson, Bonnie L., Sarkar, Sumit, 2020. Impaired amyloid beta clearance and brain microvascular dysfunction are present in the Tg-SwDI mouse model of Alzheimer's disease. Neuroscience 440, 48–55.

Sahin, Adem, YÖYen ErmİŞ, Diğdem, Caban, Secil, Horzum, Utku, Aktaş, Yeşim, Couvreur, Patrick, Esendağlı, Güneş, Capan, Yilmaz, 2017. Evaluation of brain-targeted chitosan nanoparticles through blood-brain barrier cerebral microvessel endothelial cells. J. Microencapsulation 34, 1–15.

Salaroglio, I.C., Gazzano, E., Kopecka, J., Chegaev, K., Costamagna, C., Fruttero, R., Guglielmo, S., Riganti, C., 2018. New tetrahydroisoquinoline derivatives overcome Pgp activity in brain-blood barrier and glioblastoma multiforme in vitro. Molecules 23.

Salaroglio, Iris Chiara, Abate, Carmen, Rolando, Barbara, Battaglia, Luigi, Gazzano, Elena, Colombino, Elena, Costamagna, Costanzo, Annovazzi, Laura,

Mellai, Marta, Berardi, Francesco, Capucchio, Maria Teresa, Schiffer, Davide, Riganti, Chiara, 2019. Validation of thiosemicarbazone compounds as P-glycoprotein inhibitors in human primary brain-blood barrier and glioblastoma stem cells. Mol. Pharm. 16, 3361–3373.

Saraiva, Cláudia, Praça, Catarina, Ferreira, Raquel, Santos, Tiago, Ferreira, Lino, Bernardino, Liliana, 2016. Nanoparticle-mediated brain drug delivery: Overcoming blood–brain barrier to treat neurodegenerative diseases. J. Control. Release 235, 34–47.

Shubbar, Maryam H., Penny, Jeffrey I., 2020. Therapeutic drugs modulate ATP-Binding cassette transporter-mediated transport of amyloid beta(1–42) in brain microvascular endothelial cells. Eur. J. Pharmacol. 874, 173009.

Sonali, Rahul Pratap, Singh, Nitesh Singh, Sharma, Gunjan, Vijayakumar, Mahalingam R., Koch, Biplob, Singh, Sanjay, Singh, Usha, Dash, Debabrata, Pandey, Bajarangprasad L., Muthu, Madaswamy S., 2016. Transferrin liposomes of docetaxel for brain-targeted cancer applications: formulation and brain theranostics. Drug Deliv. 23, 1261–1271.

Tapeinos, Christos, Battaglini, Matteo, Ciofani, Gianni, 2017. Advances in the design of solid lipid nanoparticles and nanostructured lipid carriers for targeting brain diseases. J. Control. Release 264, 306–332.

Tashima, T., 2020. Smart strategies for therapeutic agent delivery into brain across the blood-brain barrier using receptor-mediated transcytosis. Chem. Pharm. Bull. (Tokyo) 68, 316–325.

Tsou, Y.H., Zhang, X.Q., Zhu, H., Syed, S., Xu, X., 2017. Drug Delivery to the brain across the blood-brain barrier using nanomaterials. Small 13.

Verscheijden, L.F.M., van Hattem, A.C., Pertijs, J.C.L.M., de Jongh, C.A., Verdijk, R.M., Smeets, B., Koenderink, J.B., Russel, F.G.M., de Wildt, S.N., 2020. Developmental patterns in human blood–brain barrier and blood–cerebrospinal fluid barrier ABC drug transporter expression. Histochem. Cell Biol.

Warren, Mark S., Zerangue, Noa, Woodford, Katie, Roberts, Lori M., Tate, Emily H., Feng, Bo, Li, Cheryl, Feuerstein, Thomas J., Gibbs, John, Smith, Bill, de Morais, Sonia M., Dower, William J., Koller, Kerry J., 2009. Comparative gene expression profiles of ABC transporters in brain microvessel endothelial cells and brain in five species including human. Pharmacol. Res. 59, 404–413.

Weksler, Babette, Romero, Ignacio A., Couraud, Pierre-Olivier, 2013. The hCMEC/D3 cell line as a model of the human blood brain barrier. Fluids Barriers CNS 10, 16.